Electronic Supplementary Information

Ag-nanoparticles-decorated ZnO Porous-nanosheets Grafted on Carbon Fiber Cloth as Effective SERS Substrates

Zhiwei Wang, [†] *Guowen Meng,* [*,†,‡] *Zhulin Huang,* [†] *Zhongbo Li,*[†] *Qitao Zhou*[†]

[†]Key Laboratory of Materials Physics, and Anhui Key Laboratory of Nanomaterials and Nanotechnology, Institute of Solid State Physics, Chinese Academy of Sciences, Hefei, 230031, China

[‡]University of Science and Technology of China, Hefei, 230026, China

[*]To whom correspondence should be addressed,

Tel: (86) 0551-65592749, Fax: (86) 0551-65591434, E-mail: gwmeng@issp.ac.cn.

The Supporting Information includes:

Part S1. Characterization of ZnO-seeds@CFC.
Part S2. Lattice-resolved TEM image of ZnO-mesoporous-NS.
Part S3. XRD patterns of ZnO-mesoporous-NSs@CFC and bare CFC.
Part S4. Adsorption capacity of different substrates.
Part S5. The photos of each stage.
Part S6. EDS characterization of Ag-NPs@ZnO-mesoporous-NSs@CFC.
Part S7. Lattice-resolved TEM image of Ag-NPs@ZnO-mesoporous-NS.
Part S8. UV-vis spectra.
Part S9. The enhancement contribution of ZnO.
Part S10. Calculation of the average enhancement factor (EF).
Part S11. SERS-signal uniformity of Ag-NPs@ZnO-mesoporous-NSs@CFC.
Part S12. Raman spectrum of CFC.

Part S1. characterization of ZnO-seeds@CFC.

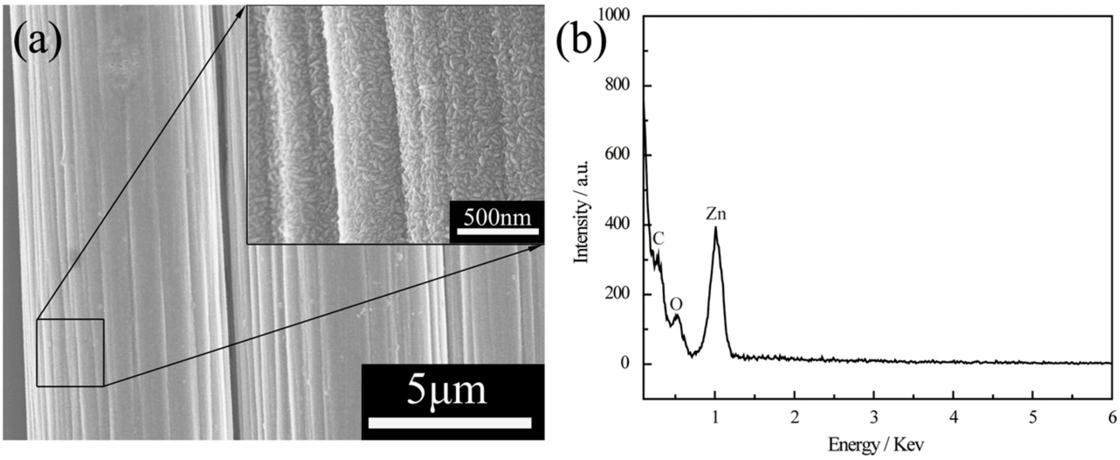

Fig. S1. (a) Typical SEM images of ZnO-seeds@CFC; (b) Energy dispersive X-ray spectrum (EDS) performed on the ZnO-seeds@CFC.

Part S2. Lattice-resolved TEM image of ZnO-mesoporous-NS.

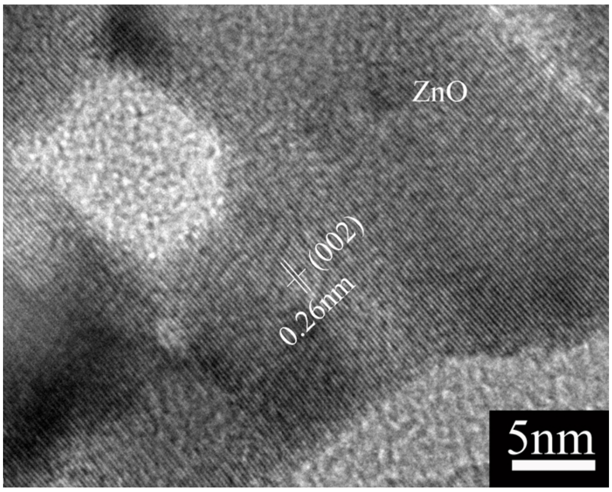

Fig. S2. lattice-resolved TEM image of ZnO-mesoporous-NS.

Part S3. XRD patterns of ZnO-mesoporous-NSs@CFC and bare CFC.

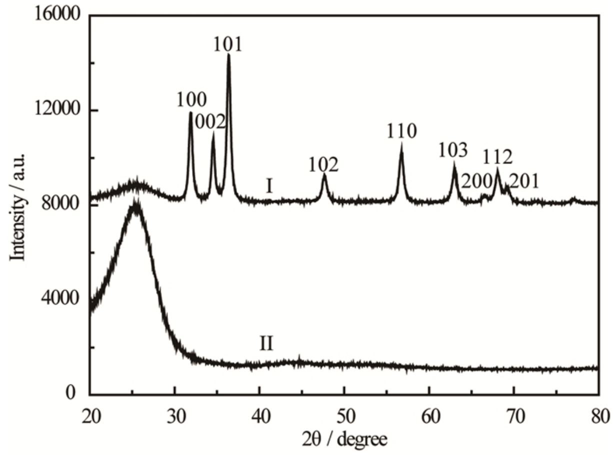

Fig. S3. XRD patterns of I: ZnO-mesoporous-NSs@CFC; II: bare CFC.

Part S4. Adsorption capacity of different substrates.

As ZnO seeds have completely covered on the surface of CFC, it indeed formed a solid and nonporous ZnO film on the surface of CFC. Therefore ZnO-seeds@CFC were used as control experimental examples to examine the impact of porous structure. The same size of CFC, ZnO-seeds@CFC, ZnO-mesoporous-NSs@CFC substrates were put into same volume of 10^{-5} M R6G solution for 12 hours respectively and then their remnant concentration were examined through UV-vis spectroscopy. Fig. S4 shows that the absorbance of the R6G solution decreased significantly with ZnO-mesoporous-NSs@CFC dipped inside, indicating that ZnO-NSs@CFC with porous structure have the highest adsorption capacity.

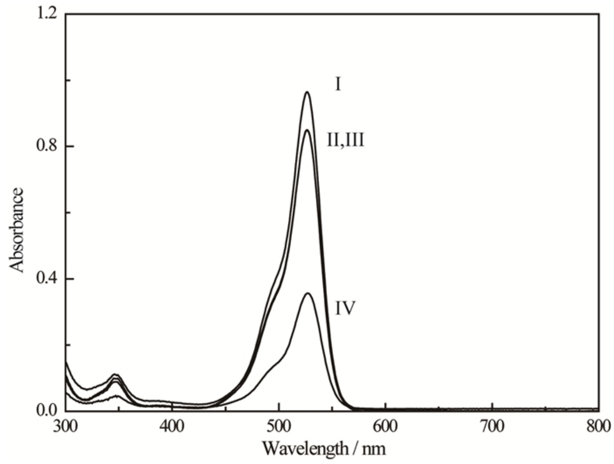

Fig. S4. UV-vis spectra of I: original 10^{-5} M R6G solution; II: R6G solution with CFC; III: R6G solution with ZnO-seeds@CFC; IV: R6G solution with ZnO-mesoporous-NSs@CFC.

Part S5. The photos of each stage.

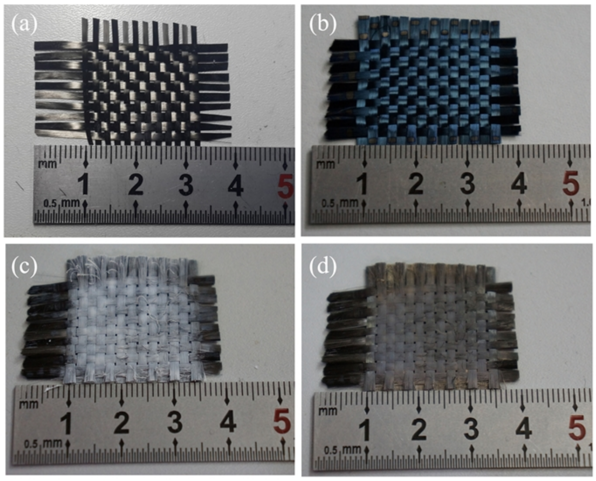

Fig. S5. The photo of (a) black CFC; (b) light-blue ZnO-seeds@CFC; (c) white ZnO-mesoporous-NSs@CFC; (d) gray Ag-NPs@ZnO-mesoporous-NSs@CFC.

Part S6. EDS characterization of Ag-NPs@ZnO-mesoporous-NSs@CFC.

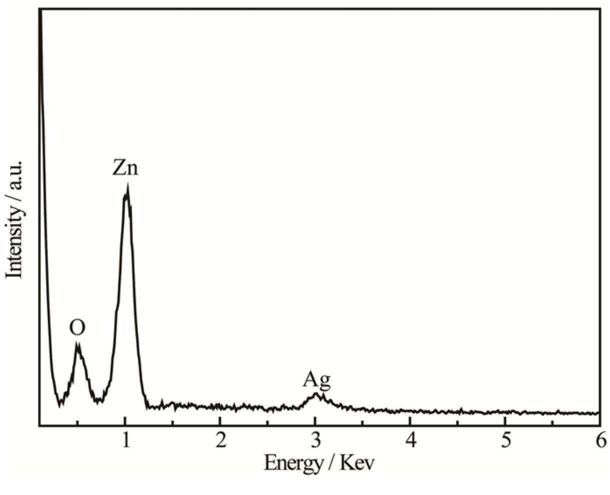

Fig. S6. EDS performed on the optimal Ag-NPs@ZnO-mesoporous-NSs@CFC.

Part S7. Lattice-resolved TEM image of Ag-NPs@ZnO-mesoporous-NS.

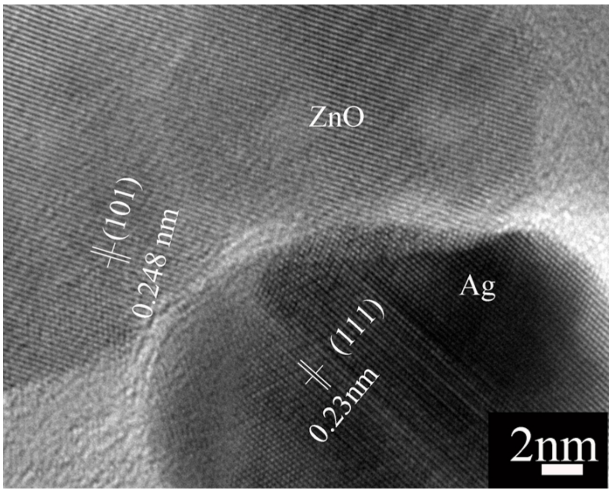

Fig. S7. Lattice-resolved TEM image of Ag-NPs@ZnO-mesoporous-NS.

Part S8. UV-vis spectra.

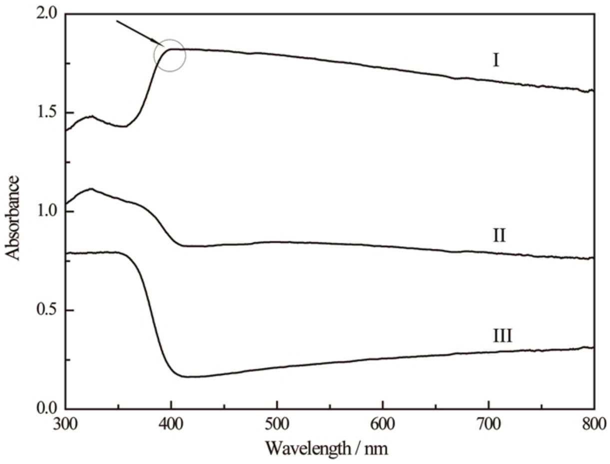

Fig. S8. UV-vis spectra of I: The difference spectrum of Ag-NPs@ZnO-mesoporous-NSs@CFC and ZnO-mesoporous-NSs@CFC; II: Ag-NPs@ZnO-mesoporous-NSs@CFC; III: ZnO-mesoporous-NSs@CFC.

Part S9. The enhancement contribution of ZnO.

To evaluate the existence of chemical enhancements from ZnO, the SERS spectra of p-ATP with different concentrations adsorbed on the ZnO-mesoporous-NSs@CFC are shown in Fig. S9. For 10^{-3} M p-ATP, four fingerprint peaks of p-ATP at 1085 cm^{-1}, 1143 cm^{-1}, 1456 cm^{-1} and 1586 cm^{-1} can be clear seen in Fig. S9(a) curve I. While for 10^{-4} M p-ATP, the fingerprint peaks of p-ATP can still be distinguished, but not so obvious, as shown in Fig. S9(a) curve II. So we further design some indirect experiments to examine its existence according to a previous work[1]. In detail, CFC, ZnO-seeds@CFC, and $Zn_4(CO_3)(OH)_6 \cdot H_2O$-NSs@CFC with the same Ag sputtering durations were used as experimental examples. Their SERS-activity to 10^{-4} M p-ATP are shown in Fig. S9(b). It is clear that Raman signal intensities of p-ATP adsorbed on the surface of Ag-NPs@ZnO-mesoporous-NSs@CFC are the largest. Although Raman signal of 10^{-4} M p-ATP adsorbed on pure ZnO-mesoporous-NSs@CFC is weak, as the $Zn_4(CO_3)(OH)_6 \cdot H_2O$-NSs have similar sheet-like structures with that of ZnO-mesoporous-NSs, the larger SERS-activity of Ag-NPs@ZnO-mesoporous-NSs@CFC than that of Ag-NPs@$Zn_4(CO_3)(OH)_6 \cdot H_2O$-NSs@CFC should be related to the contribution of ZnO.

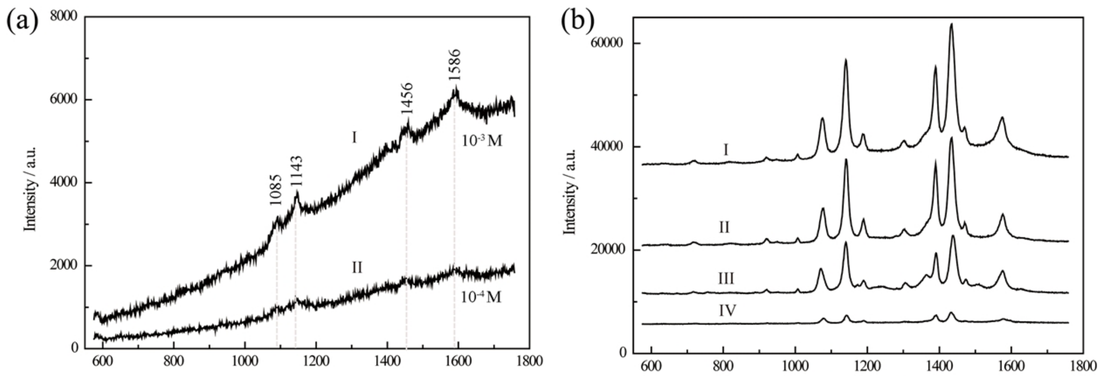

Fig. S9. (a) SERS spectra of p-ATP with different concentrations adsorbed on the ZnO-mesoporous-NSs@CFC. I: 10^{-3} M p-ATP; II 10^{-4} M p-ATP. (b) SERS spectra of 10^{-4} M p-ATP by using I: Ag-NPs@ZnO-mesoporous-NSs@CFC; II: Ag-NPs@$Zn_4(CO_3)(OH)_6 \cdot H_2O$-NSs@CFC; III: Ag-NPs@ZnO-seeds@CFC; IV: Ag-NPs@CFC.

Part S10. Calculation of the average enhancement factor (EF).

The EF can be calculated by

$$EF = \frac{I_{SERS}/N_{SERS}}{I_{Nor}/N_{Nor}}$$

Where I_{SERS} and I_{Nor} represent the intensity of the 1600 cm^{-1} band in the Raman spectrum of p-ATP and normal Raman spectrum, under the same experimental conditions (laser wavelength, laser power, microscope objective/lenses, accumulation time), respectively. N_{SERS} and N_{Nor} represent the corresponding number of molecules in the focused incident laser spot. Herein, for SERS experiment, a certain volume (V_{SERS}) and concentration (C_{SERS}) p-ATP ethanol solution was dispersed to an area of S_{SERS} at the as-fabricated substrate. Similarly, for normal Raman experiment, a certain volume (V_{Nor}) and concentration (C_{Nor}) p-ATP ethanol solution was dispersed to an area of S_{Nor} at a clean glass substrate. Both the substrates were dried in air. Thus the foregoing equation can be rewritten as follows:

$$EF = \frac{I_{SERS}}{I_{Nor}} \bullet \frac{S_{SERS}V_{Nor}C_{Nor}}{S_{Nor}V_{SERS}C_{SERS}}$$

In our experiments, 70 μL 10^{-3} M p-ATP ethanol solution was dispersed to an area of about 50 mm^2 on a glass substrate，40 μL 10^{-9} M p-ATP ethanol solution was dispersed to an area of about 60 mm^2 for the Ag-NPs@ZnO-mesoporous-NSs@CFC and 40 μL 10^{-7} M p-ATP ethanol solution was dispersed to an area of about 70 mm^2 for the Ag-NPs@ZnO-seeds@CFC. Fig. S10(a) and S10(b) show the Raman spectrum of p-ATP from the above-mentioned substrates. For the band at 1600 cm^{-1}, I_{SERS}/I_{Nor} is about 2.66 and 1.66. Hence the average enhancement factor for Ag-

NPs@ZnO-mesoporous-NSs@CFC and Ag-NPs@ZnO-seeds@CFC are calculated to be 5.58×10^6 and 4.06×10^4.

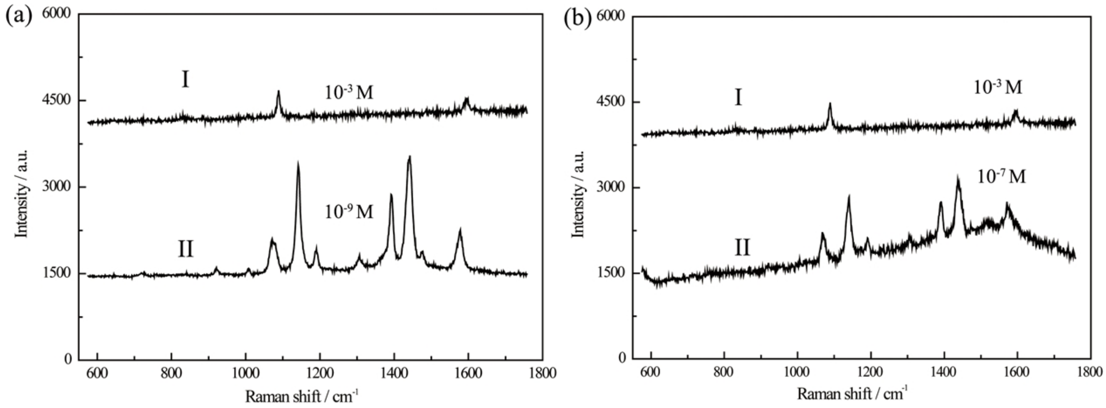

Fig. S10. (a) I: Raman spectrum of p-ATP obtained using dried 70 μL 10^{-3} M PATP ethanol solution dispersed on 50 mm^2 glass substrate. II: SERS spectrum of 40 μL 10^{-9} M p-ATP ethanol solution dispersed on 60 mm^2 Ag-NPs@ZnO-mesoporous-NSs@CFC (b) I: Raman spectrum of p-ATP obtained using dried 70 μL 10^{-3} M PATP ethanol solution dispersed on 50 mm^2 glass substrate. II: SERS spectrum of 40 μL 10^{-7} M p-ATP ethanol solution dispersed on 70 mm^2 Ag-NPs@ZnO-seeds@CFC.

Part S11. SERS-signal uniformity of Ag-NPs@ZnO-mesoporous-NSs@CFC.

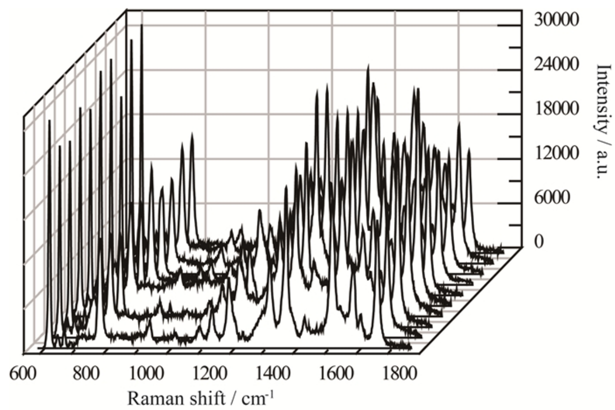

Fig. S11. SERS spectra of R6G obtained from ten random carbon fibers of as-prepared optimal SERS substrate. Data acquisition time 5 s, [R6G] = 1.0×10^{-7} M.

Part S12. Raman spectrum of CFC.

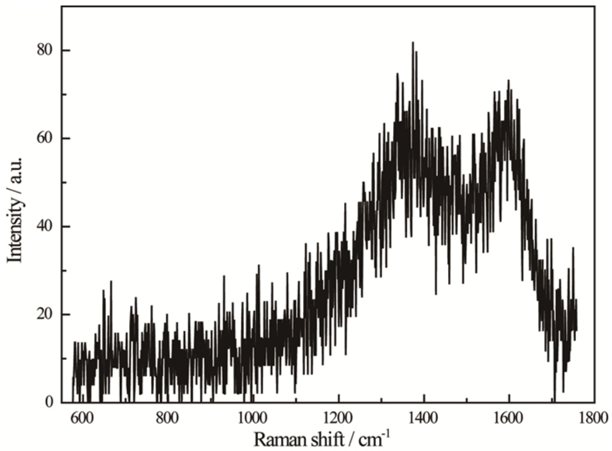

Fig. S12. Raman spectrum of CFC.

References

1 L. Yang, W. Ruan, X. Jiang, B. Zhao, W. Xu and J. R. Lombardi, *J. Phys. Chem. C* 2009, ***113***, 117-120.